Hindawi Publishing Corporation
International Journal of Rotating Machinery
Volume 2016, Article ID 9306314, 11 pages
http://dx.doi.org/10.1155/2016/9306314

Research Article

Numerical Investigation of Pressure Fluctuation Characteristics in a Centrifugal Pump with Variable Axial Clearance

Lei Cao, Zhengwei Wang, Yexiang Xiao, and Yongyao Luo

State Key Laboratory of Hydroscience and Engineering and Department of Thermal Engineering, Tsinghua University, Beijing 100084, China

Correspondence should be addressed to Zhengwei Wang; wzw@mail.tsinghua.edu.cn

Received 9 December 2015; Revised 22 March 2016; Accepted 5 April 2016

Academic Editor: Jiun-Jih Miau

Clearance flows in the sidewall gaps of centrifugal pumps are unsteady as well as main flows in the volute casing and impeller, which may cause vibration and noise, and the corresponding pressure fluctuations are related to the axial clearance size. In this paper, unsteady numerical simulations were conducted to predict the unsteady flows within the entire flow passage of a centrifugal pump operating in the design condition. Pressure fluctuation characteristics in the volute casing, impeller, and sidewall gaps were investigated with three axial clearance sizes. Results show that an axial clearance variation affects the pressure fluctuation characteristics in each flow domain by different degree. The greatest pressure fluctuation occurs at the blade pressure surface and is almost not influenced by the axial clearance variation which has a certainly effect on the pressure fluctuation characteristics around the tongue. The maximum pressure fluctuation amplitude in the sidewall gaps is larger than that in the volute casing, and different spectrum characteristics show up in the three models due to the interaction between the clearance flow and the main flow as well as the rotor-stator interaction. Therefore, clearance flow should be taken into consideration in the hydraulic design of centrifugal pumps.

1. Introduction

Unsteady flows in centrifugal pumps are always paid attention to in engineering, which can cause vibration, noise, and even fatigue failure. Pressure fluctuation is one of the most common phenomena of unsteady flows. Considerable investigations [1–12] have been performed on pressure fluctuation characteristics in volute casings and impellers of centrifugal pumps, concluding that blade-tongue interaction plays a dominant role in causing fluctuating main flows, and the influencing factors including flow rate and impeller-tongue gap size have been analyzed. But flows in sidewall gaps, which refer to the space between impeller shrouds and casing covers, are usually ignored. However, Uy and Brennen [13] found that the leakage path had considerable influence on the rotor dynamic force when they did some experiments for centrifugal pumps whose shrouds were in different shapes. Increasing scholars are paying attention to the clearance flows in centrifugal pumps in recent years. Spence and Amaral-Teixeira [14] carried out an unsteady numerical simulation for a double suction pump and thought that the deviation in pressure fluctuations between the numerical and experimental results was due to the simplified front shroud in the simulation. Park and Morrison [15] probed into the interaction between the back clearance flow and impeller passage flow by calculating the pressure fluctuations in a centrifugal pump with a semiopen impeller. Pei et al. [16–19] claimed the unstable flow in the sidewall gaps could not be ignored for the sake of an accurate calculation and analysis of the pressure fluctuation intensity and turbulence intensity distribution in the entire flow passage of a single-blade centrifugal pump. In addition, the size of the leakage path has certain influence on the main flow field. Radial clearance sizes, usually referring to wear ring sizes, were studied in a centrifugal pump by Liu et al. [20] and they found that the velocity and pressure distribution in the front wear ring was related to its radial dimension. Many scholars [21–24] also experimentally and theoretically discovered that changing the distance between a rotating wall and a stationary wall would make the flow structure between the two walls show different characters. However,

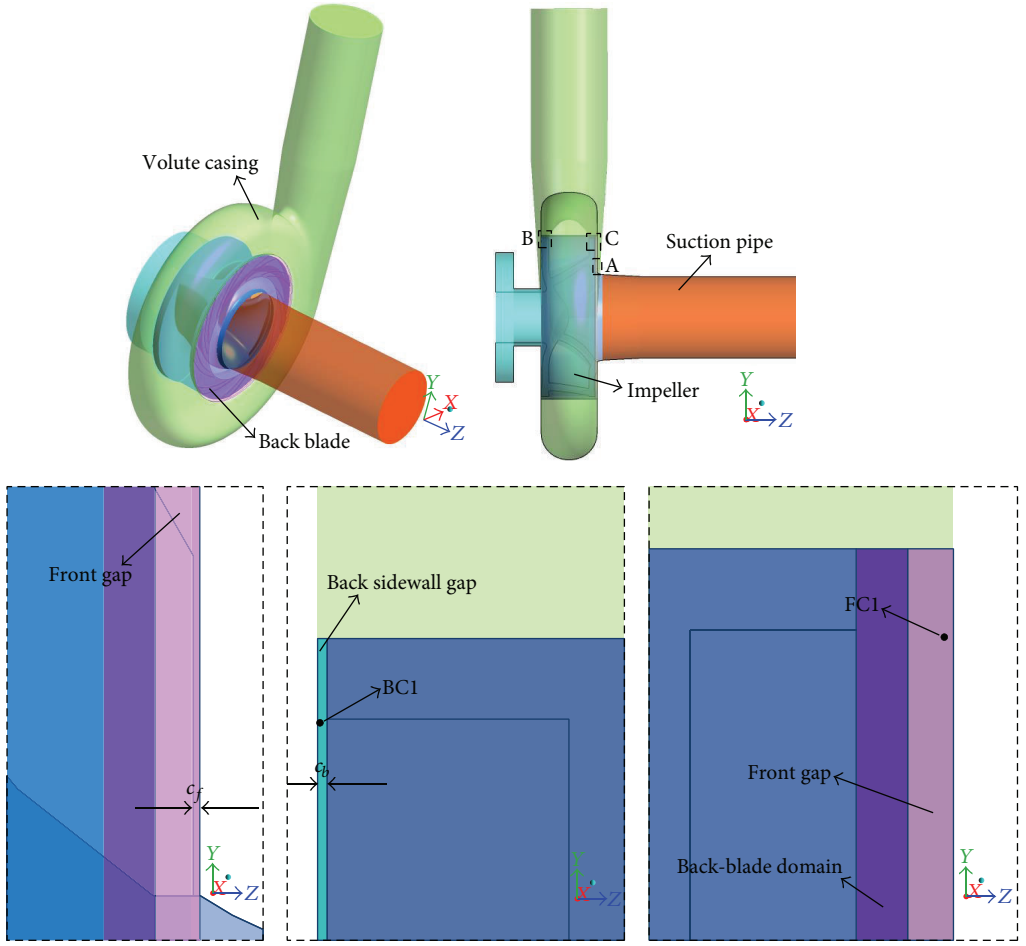

Figure 1: Geometry of the centrifugal pump.

little research has been done to analyze the influence of axial clearance sizes on the unsteady flow characteristics in centrifugal pumps. Therefore, it is meaningful to discuss the effect of axial clearance sizes on the pressure fluctuations in centrifugal pumps, which will facilitate the optimal design and safe operation of centrifugal pumps.

In this paper, unsteady numerical simulations were carried out in the design condition for the entire flow passage of a centrifugal pump. Three axial clearance sizes were obtained by moving the impeller along the axial direction. The numerical codes were first validated by a model test. Then we analyzed the pressure fluctuation characteristics in each flow domain and gave an understanding on how axial clearance sizes influenced the unsteady flows in centrifugal pumps.

2. Numerical Method

2.1. Physical Model and Grid. The centrifugal pump studied in this paper has a shrouded impeller with nine back blades on the front shroud, whose basic parameters are given in Table 1. The 3D entire flow passage, including suction pipe, impeller, volute casing, front sidewall gap, and back sidewall gap, was built by the 3D modeling software UG NX 6.0. The actual front sidewall gap was divided into two domains, the rotating back-blade domain and the stationary front gap (the front gap mentioned below refers to this stationary part), to better predict the flow field affected by the rotating back blades. Figure 1 shows the 3D view of the entire computational domain and the axial section with partial enlarged views of the front clearance and back clearance. The impeller can move in the axial direction between the front casing cover and the back casing cover; the front axial clearance size c_f and the back axial clearance size c_b conform to the expression $c_f + c_b = 1$ mm.

Four pump models listed in Table 2 were chosen to be numerically investigated to discuss the correlation between axial clearance sizes and unsteady flow characteristics. M1, M2, and M3 are models with front and back sidewall gaps; M4 is a model similar to M3 but only contains three main flow domains, that is, suction pipe, impeller, and volute casing.

Structure grids were generated for all domains except impeller. Unstructured tetrahedron elements were used in impeller due to its three-dimensional twisted blades. Grid refinement was processed near the blade surfaces. Steady simulations were conducted for Model M2 in the design condition with four different mesh densities, total element number from 0.9 million to 2.0 million. The results with

Table 1: Basic parameters of the pump.

Parameter	Value
Impeller inlet diameter	$D_0 = 85$ mm
Impeller outlet diameter	$D_2 = 310$ mm
Blade number	$Z_1 = 3$
Blade inlet angle	$\beta_1 = 44^\circ$
Blade outlet angle	$\beta_2 = 29^\circ$
Blade outlet width	$B = 79.2$ mm
Back-blade number	$Z_2 = 9$
Back-blade width (axial direction)	$b = 1.9$ mm
Back-blade inlet angle	$\beta_{b1} = 19^\circ$
Back-blade outlet angle	$\beta_{b2} = 26^\circ$
Volute casing width at impeller outlet	$B_v = 110$ mm
Blade-tongue gap	$\Delta d = 0.29D_2$
Specific speed*	$n_s = 165$
Design flow rate	$Q_0 = 0.08\ \mathrm{m}^3/\mathrm{s}$
Design head	$H_0 = 11.3$ m

*Specific speed is defined as $n_s = 3.65nQ_0^{1/2}/H_0^{3/4}$, where n is the rated rotational speed, r/min. The unit of n_s is usually ignored.

Table 2: Research models.

Model	c_f (mm)	c_b (mm)
M1	0.22	0.78
M2	0.42	0.58
M3	0.62	0.38
M4	None	None

1.63 million or more elements had little difference. Thus, the grid scheme with 1.63 million elements was chosen to balance the calculation accuracy and cost. Grids for the four models have similar topological structure, with almost the same amount of elements in the volute casing, impeller, and suction pipe; the element amount of sidewall gaps proportionally changes with the variation of axial clearance sizes. Figure 2 shows the grid of back sidewall gap, back-blade domain, and front gap of Model M2, with partial enlarged views.

2.2. Numerical Method and Boundary Condition. With commercial CFD software package ANSYS CFX14.5, we used Reynolds-Averaged Navier-Stokes (RANS) equations to calculate the incompressible turbulent flow in the centrifugal pump. For better prediction of flow separation and rotational flows, SST k-ω turbulence model with automatic wall function was applied to close the governing equations. After checking timestep independence, the timestep was set as 1/150 of one revolution; that is, the impeller rotates 2.4° after each timestep. During each timestep, the code keeps running until the iteration residual drops to 0.0001.

A total pressure was specified at the suction pipe inlet and a mass flow rate was specified at the volute casing outlet. The impeller and back-blade domain had the same rotational speed, 1000 r/min, and other domains were all set to be stationary. Steady simulations were first carried out and then the results were used as the initial flow fields for unsteady simulations. In steady simulations, the interface between rotor and stator adopted Frozen Rotor Model, while in unsteady simulations it used Transient Frozen Rotor Model. The Frozen Rotor Model treats the flow from one component to the next by changing the frame of reference and maintaining the relative position of the components, while the Transient Rotor-Stator Model, which considers all interaction effects between components that are in relative motion to each other, updates the transient relative motion between the components on each side of the interface every timestep [25]. Walls were all set as no-slip walls. In front and back sidewall gaps, the walls contacting front or back shrouds were set as rotational walls that had the same speed of impeller.

Unsteady numerical simulations were processed with design flow rate Q_0 for models M1, M2, and M3. When the calculations became stable, we continued the calculation for another six periods. The data of the last six periods are used to obtain the pump performance. Pressure variations were also recorded at several locations within the entire flow passage during the last six periods. Pressure fluctuations in the volute casing were studied via Points VC0~VC8 and in the impeller via Points BP1~BP5 located on the pressure surface and Points BS1~BS5 located on the suction surface. These points are all on the middle section of the volute casing as shown in Figure 3(a). In the front and back sidewall gaps, pressure fluctuations at Points FC1~FC4 and BC1~BC4 as shown in Figure 3(b) were analyzed, respectively. The axial and radial positions of these points are illustrated in Figure 1 (0.15 mm away from the casing cover).

2.3. Validation of Simulation Results. Validation of the numerical method is conducted by comparing with the corresponding model test results from Zhang's master thesis [26]. The model test was conducted in a closed hydraulic machinery test rig whose essential measuring equipment has been introduced in our previous work [27]. Flow rate was measured by an intelligent electromagnetic flowmeter with an uncertainty of ±0.2%. Head was measured by an intelligent differential pressure transmitter with an uncertainty of ±0.1%. Torque was measured by intelligent torque and rotational speed transducer with an uncertainty of ±0.1%. The rotational speed of the test pump was 1000 r/min as in the simulation. The efficiency was calculated with the time-averaged head and axial power. Meanwhile, pressure data were recorded through CGYL-201 high-precision hydraulic pressure fluctuation transducers which were flush-mounted on the casing wall at Point VC5. The uncertainty of the pressure transducer is ±0.5% and the dynamic response range is from 0 to 1500 Hz. The experimental sampling frequency was 4096 Hz and the sampling duration was 20 s for each condition.

Experimental and numerical results of the efficiency and head in the design condition are given in Table 3. When considering sidewall gaps, that is, for M1, M2, and M3, the relative errors are all within 5%, and the error rises as c_f increases. This may be related to the complicated flow states in the front sidewall gaps. Experimental and numerical results

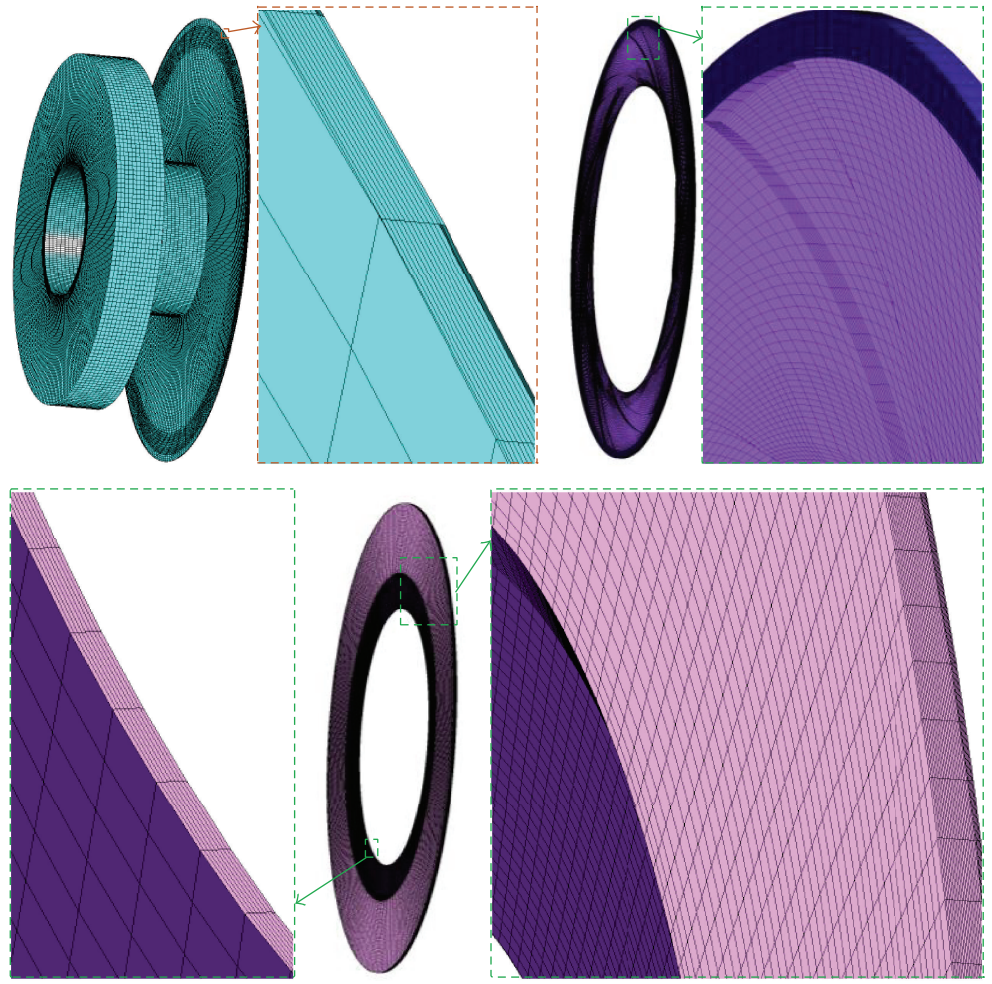

Figure 2: Grid of the sidewall gaps.

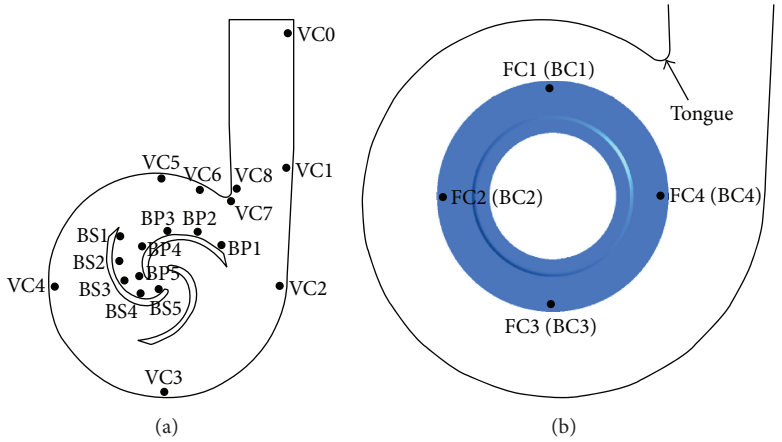

Figure 3: Distribution of pressure recording points.

exhibit a similar trend: the efficiency and head both drop as c_f increases. In our previous study [27], it has been found that as c_f increases, the interaction between the clearance flow and the main flow becomes stronger, leading to a decline of the simulation accuracy. The error would be larger if the sidewall gaps were ignored in the simulation. The relative error of the efficiency of M4 is over 10% since it does not take volumetric losses and mechanical losses into account and moreover it is hard to reflect the hydraulic losses caused by the interaction between the clearance flow and the main flow.

Table 3: Comparison of numerical results with experiment results of the pump performance.

	Efficiency			Head		
	Experiment (%)	Simulation (%)	Error* (%)	Experiment (m)	Simulation (m)	Error* (%)
M1	82.8	83.0	0.24	11.45	11.36	−0.79
M2	81.0	82.6	1.98	11.30	11.33	0.44
M3	78.3	81.8	4.47	10.88	11.23	3.22
M4	78.3	86.7	10.73	10.88	10.34	−4.96

*Error = |simulation result − experiment result|/(experiment result) 100%.

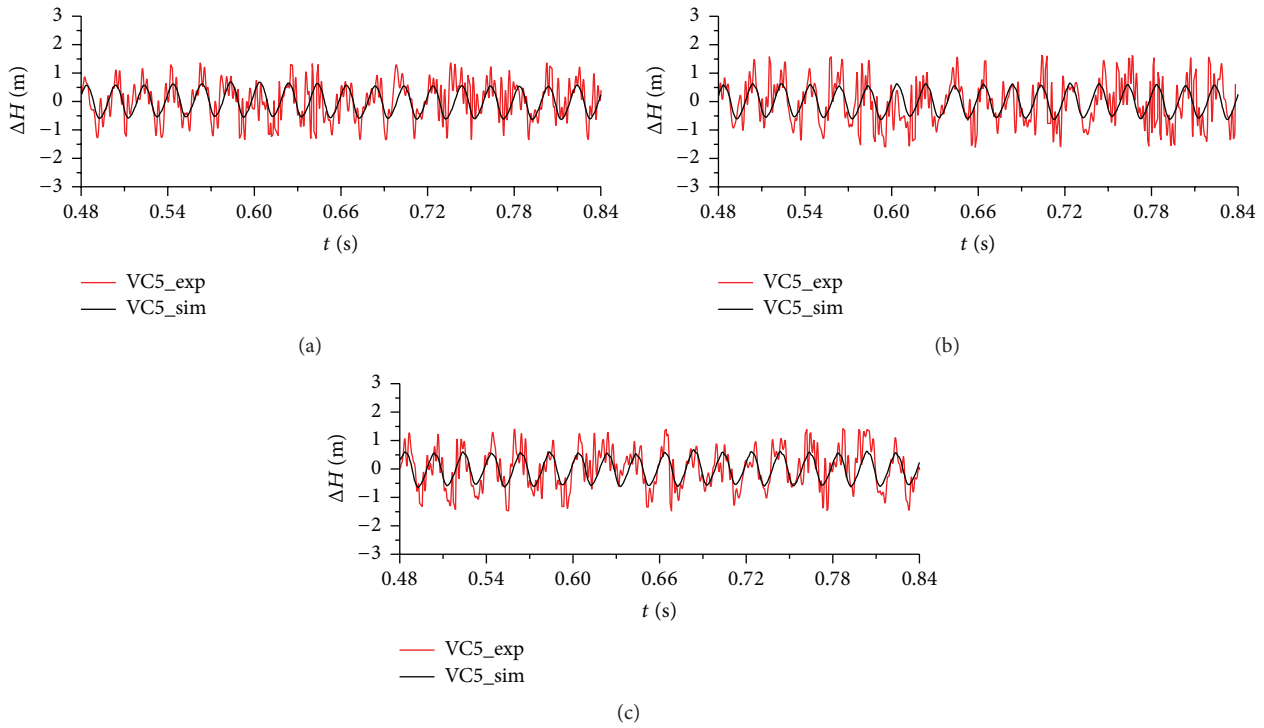

Figure 4: Comparison of the experimental and numerical pressure variations in three models: (a) M1, (b) M2, and (c) M3.

Pressure fluctuation data obtained by the numerical simulations and model test are compared for M1, M2 and M3. Relative pressure was got by subtracting the average pressure of six periods. We take 97% confidence interval for both numerical and experimental data to avoid unreliable data. Pressure variations with time are displayed in Figure 4. The numerical results show similar patterns as the experimental results except that the predicted peak-peak amplitudes are slightly smaller than the experiment results and the numerical simulations are not able to predict the small high-frequency undulations. Fast Fourier Transform (FFT) was conducted for the pressure data and the frequency spectrums are presented in Figure 5. Numerical results are in high agreement with experimental results at dominant frequency, but the numerical secondary-frequency amplitudes are smaller than the experimental ones especially at low frequencies.

The comparison shown in Figures 4 and 5 in both external performance and pressure fluctuation data demonstrates that the numerical method used in this paper meets the accuracy requirement. Then this numerical method is applied to investigate the pressure fluctuation characteristics in the centrifugal pump with different axial clearance sizes.

3. Results and Discussion

3.1. Pressure Fluctuations in the Main Flow Region

3.1.1. Volute Casing. Unsteady flow in volute casings is always a research hotspot for centrifugal pumps. For this pump, the strongest pressure fluctuation in the volute casing occurs around the tongue, which is consistent with the conclusions of many previous studies. From Figure 6 (the vertical coordinate denotes the ratio of the pressure fluctuation peak-peak amplitude and the corresponding pump head), the peak-peak amplitude first decreases along the flow direction (counterclockwise from Point VC7 to Point VC3) and then rises in the diffusing section (from Point VC2 to Point VC0). The blade-tongue interaction affects the flow field in the tongue region

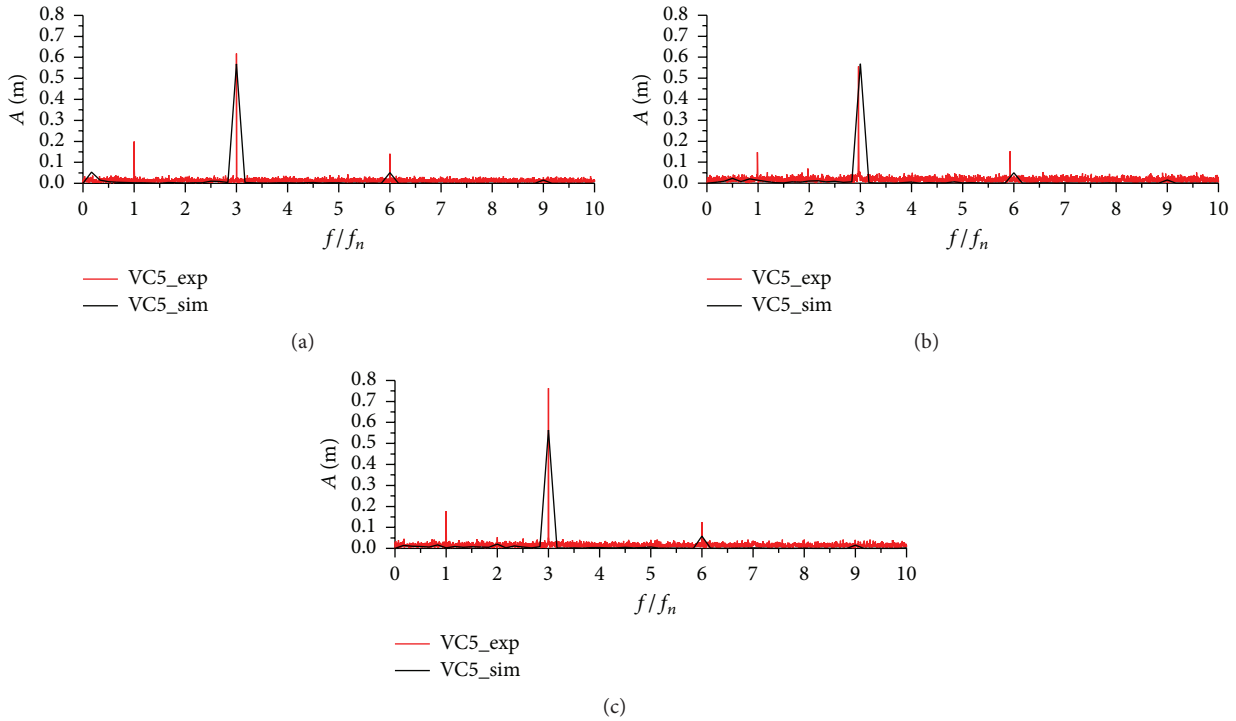

Figure 5: Comparison of the experimental and numerical frequency spectrum in three models: (a) M1, (b) M2, and (c) M3. f_n denotes rotating frequency.

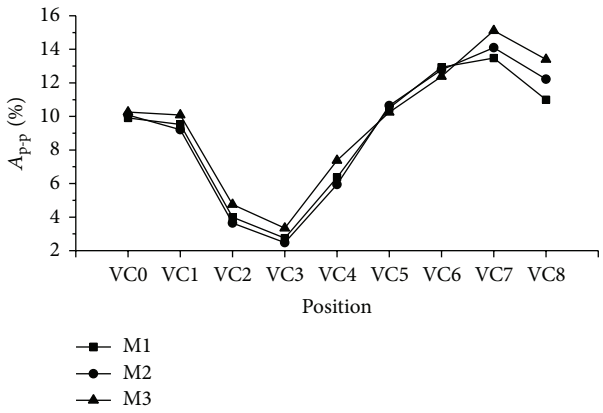

Figure 6: Peak-peak amplitudes at the points in the volute casing.

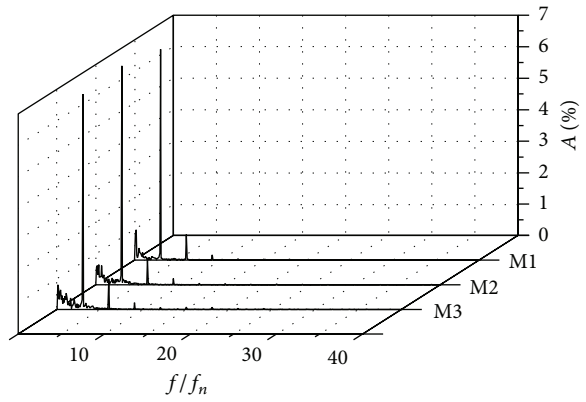

Figure 7: Frequency spectrum of the pressure fluctuations at Point VC7.

and causes stronger pressure fluctuations around the tongue; as the pressure wave propagates away from the tongue, the pressure fluctuation amplitude decreases. An axial clearance variation has little influence for most points in the volute casing; as c_f increases, the peak-peak amplitude only has an evident rise at the points near the tongue, that is, Point VC7 and Point VC8.

Via FFT algorithm, we find that the dominant frequency at every point in the volute casing is all triple rotating frequency, that is, blade passing frequency, which again proves the effect of the blade-tongue interaction. Figure 7 compares the frequency spectrum at Point VC7 for the three models. The amplitude at the dominant frequency is nearly not influenced by the axial clearance variation, only with a slightly higher value in M2. There are rich low-frequency components at Point VC7 which may be related to the complicated vortex structures around the tongue, and a larger c_f leads to richer low-frequency components. The vorticity distribution on the middle section of the pump exhibited in Figure 8 confirms the above conclusion. The increasing c_f results in more nonuniform vorticity distribution. It is related to the interference of the front clearance flow to the main flow, which is particularly severe near the tongue due to the rotor-stator interaction. A larger c_f brings more leakage fluid and accordingly induces severer disturbance around the tongue [27].

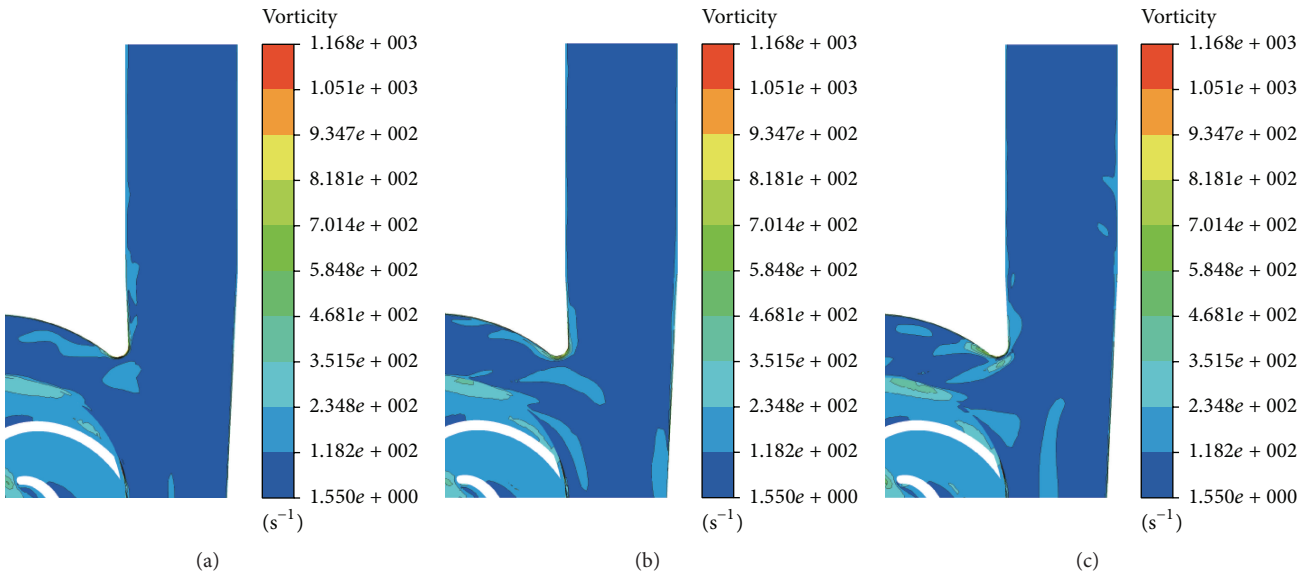

Figure 8: Vorticity distribution on the middle section: (a) M1, (b) M2, and (c) M3.

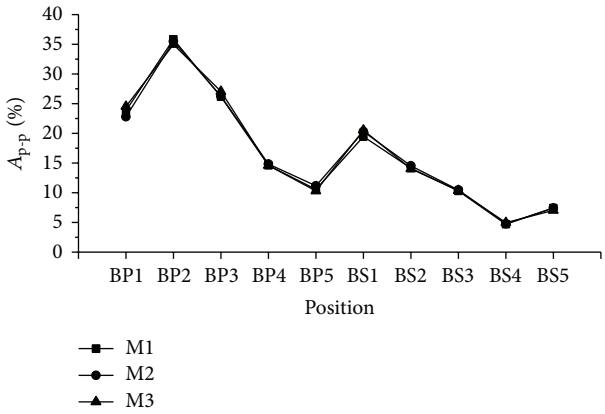

Figure 9: Peak-peak amplitudes at the points in impeller.

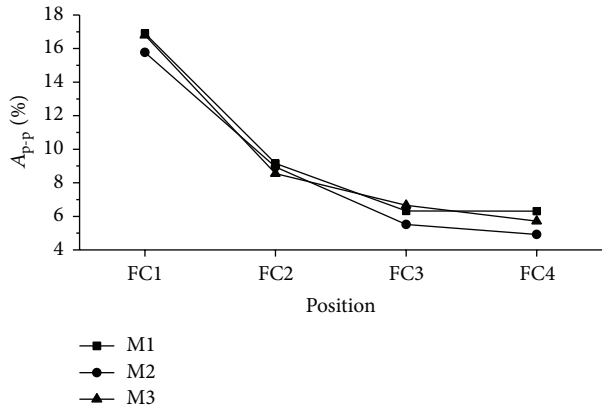

Figure 10: Peak-peak amplitude at the points in the front gap.

3.1.2. Impeller. Flow states in blade channels have significant influence on the pump performance. It is not easy to experimentally measure the flow field in rotating components, while CFD can be a good tool. Figure 9 shows the peak-peak amplitudes of the pressure fluctuations on the blade surfaces, which are larger on the pressure surface than on the suction surface. The effect of rotor-stator interaction is greater at the impeller outlet; thus the pressure fluctuation peak-peak amplitude rises from the impeller inlet to outlet. In addition, axial clearance variation has nearly no influence on the pressure fluctuations in the impeller. Based on our previous research [27], the clearance flows directly interact with the flows in the volute casing (near the impeller outlet) and in the suction pipe (just in front of the impeller inlet) rather than with the flows inside the impeller. So the clearance variation scarcely affects the pressure fluctuation characteristics in the blade channels. We also process a spectral analysis and find that the dominant frequency in the impeller is the rotating frequency induced by the blade-tongue interaction. Additionally, it demonstrates that the pressure fluctuations on the pressure surface of the blade are severer than those in the volute casing; thus the unsteady flow in the rotating domain is still a research focus in terms of the centrifugal pump flow instability.

3.2. Pressure Fluctuations in the Side Chambers. Clearance flows in sidewall gaps are often ignored. However, through numerical simulations, we find that noteworthy pressure fluctuations exist in the sidewall gaps.

3.2.1. Front Sidewall Gap. The pressure fluctuation characteristics at Points FC1~FC4 in the front gap were analyzed. The pressure fluctuation peak-peak amplitudes gradually decrease along the flow direction (counterclockwise from Point FC1 to Point FC4) and at Point FC1 it even exceeds the maximum value in the volute casing, as displayed in Figure 10. The results of M1 and M3 have little difference, but they are

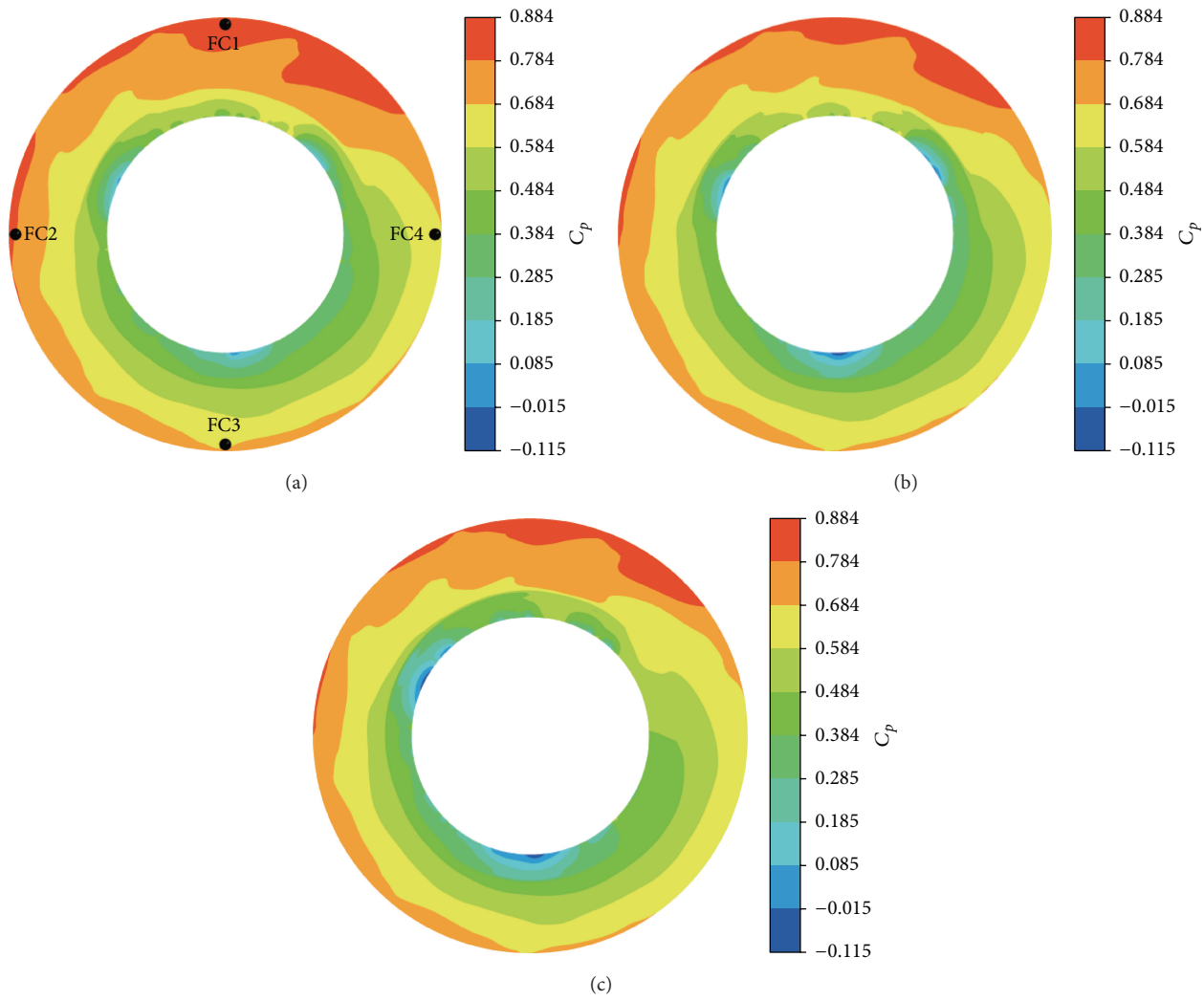

Figure 11: Pressure coefficient distribution on one section of the front gap at the last timestep: (a) M1, (b) M2, and (c) M3.

Table 4: Comparison of the dominant frequencies at the points in the front gap.

%	M1 f_d/f_n	M2 f_d/f_n	M3 f_d/f_n
FC1	3	3	3
FC2	3	3	3
FC3	9	9	9
FC4	1/6	9	3

f_d is the dominant frequency.

slightly larger than that of M2. Thus the pressure fluctuation intensity does not monotonously go up or down with the increase of c_f.

The dominant frequencies of the pressure fluctuations in the front gap are listed in Table 4. In each model, the dominate frequencies are not totally the same for the four points; the dominant frequencies at Point FC4 are also different for the three models. The clearance flow in the front gap is disturbed by the rotating component. The blade passing frequency ($3f_n$) dominates the pressure fluctuation in most region, while the back-blade passing frequency ($9f_n$) plays a more important role at some lower regions. At Point FC4 in M1, there even exists a frequency of $1/6f_n$ which may be related to the combined effect of the impeller blades and back blades. Consider the complexity of the flow states in the front gap.

Figure 11 displays the pressure coefficient distribution on the section where Points FC1~FC4 locate. The pressure coefficient is defined as $C_p = 2(p - p_{\text{inlet}})/(\rho u_2^2)$, where p_{inlet} is the area-averaged pressure at the pump inlet and u_2 is the velocity at the impeller outlet. The pressure patterns look globally similar for the three models: the pressure distribution is not circumferentially uniform with evidently higher values in the top, which confirms the effect of the uneven flows in the volute casing. In addition, as c_f increases, the pressure level slightly drops. In each model, C_p decreases from FC1 to FC4 which is consistent with the corresponding pressure fluctuation peak-peak amplitude distribution feature. It indicates that the pressure at the top region is not only with higher values but also fluctuating more greatly.

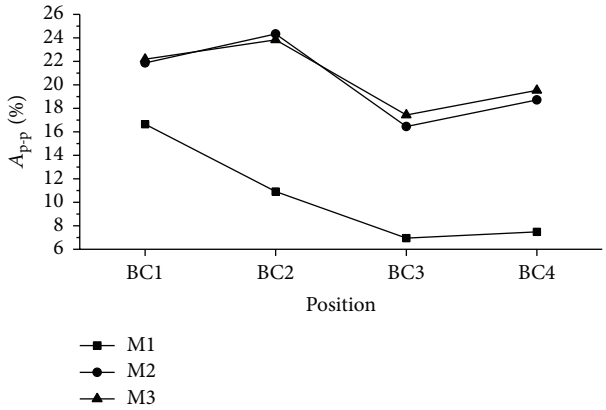

Figure 12: Peak-peak amplitudes at the points in the back sidewall gap.

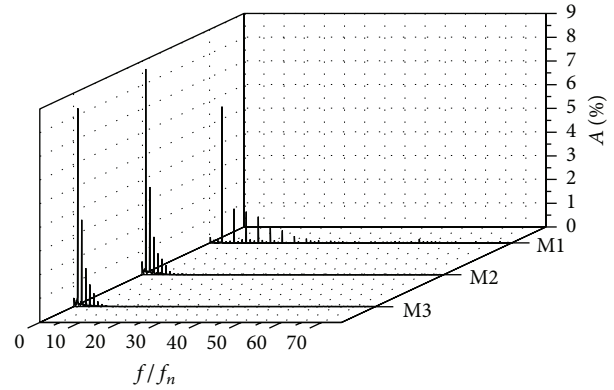

Figure 13: Frequency spectrum of the pressure fluctuations at Point BC1.

3.2.2. Back Sidewall Gap. The pressure fluctuations in the back sidewall gap evidently differ from those in the front gap. As shown in Figure 12, in M1 the peak-peak amplitudes of the pressure fluctuations at the four points in the back sidewall gap are similar to those in the front gap, while in M2 and M3 the peak-peak amplitudes are much higher and slightly undulate along the flow direction (from Point BC1 to Point BC4).

A frequency spectrum analysis indicates that the four points in the back sidewall gap of each model have the same frequency components. We take Point BC1 as an example to illustrate the effect of the axial clearance variation. Figure 13 shows the corresponding frequency spectrum. In M1 the dominant frequency is the blade passing frequency, while in M2 and M3 the dominant frequency is the rotating frequency. Due to the viscous force, the fluid in the back sidewall gap flows with the rotating back shroud. The decreasing back clearance strengthens the viscous effect; thus the pressure fluctuation is weaker in M1. For M2 and M3, the flow fields are relatively symmetric owing to the smaller back clearance, and the rotating back shroud contributes to the dominant frequency (i.e., the rotating frequency). However, in M1 there is more mass transfer between the back sidewall gap and the main flow domain; thus the pressure wave dominated by the blade passing frequency propagates to the back sidewall gap.

Figure 14 displays the pressure coefficient distribution on the section where Points BC1~BC4 locate. Compared to the pressure filed in the front gap, the pressure in the back sidewall gap distributes more evenly along the circumferential direction, and it gradually increases with the radius. Agreeing with the explanation in the last paragraph, the pressure presents more uneven pattern in M1 due to a bigger distance from the back shroud.

To sum up, the unsteady flow in the entire flow passage of the centrifugal pump is strongly associated with the rotor-stator interaction. The blade-tongue interaction is the main source of the pressure fluctuations in the main domains. Meanwhile, the front shroud, back shroud, and back blades that rotate with the impeller make the fluid in the sidewall gaps rotate at some degree, which may interact with the main flow. Flow states in the sidewall gaps are sensitive to the axial clearance size. A variation of the axial clearance affects the unsteady flow characteristics in the sidewall gaps and changes the level of the interaction between the clearance flow and the main flow, which leads to different pressure fluctuation frequencies. Flows in the impeller have no direct contact with clearance flows; thus the pressure fluctuation characteristics in the blade channels are not obviously affected by the axial clearance variation. It is meaningful to investigate the unsteady flow characteristics and the origin of the pressure fluctuations by doing numerical simulations for the entire flow passage of a centrifugal pump.

4. Conclusions

In this paper, unsteady numerical simulations were conducted in the design condition for a centrifugal pump with three axial clearance sizes, and the influence of axial clearance variation on the pressure fluctuation characteristics was analyzed for each flow domain. The numerical results of pump performance and pressure fluctuations with different axial clearance sizes all agree well with the experimental results. Through spectral analysis for several key points, we find that the axial clearance variation affects the pressure fluctuation characteristics in different flow domains by different degrees. Within the entire flow passage, the most intensive pressure fluctuation occurs at the blade pressure surface, which comes from the blade-tongue interaction, and it is almost not influenced by the axial clearance variation. The range of pressure fluctuation peak-peak amplitudes in the volute casing and in the sidewall gaps is mostly similar, but the maximum amplitude in the sidewall gaps is larger than that in the volute casing. Axial clearance sizes certainly affect the pressure fluctuation characteristics around the tongue and its effect is embodied in the low frequencies. Pressure fluctuation peak-peak amplitudes in the sidewall gaps do not change monotonously with the increase of the axial clearance size. In the front gap, the dominant frequency is not the same value for the four points in each model and also for the same point in different models. In the back sidewall gap, the largest back axial clearance leads to a much smaller pressure fluctuation which is related to viscous force from the rotating

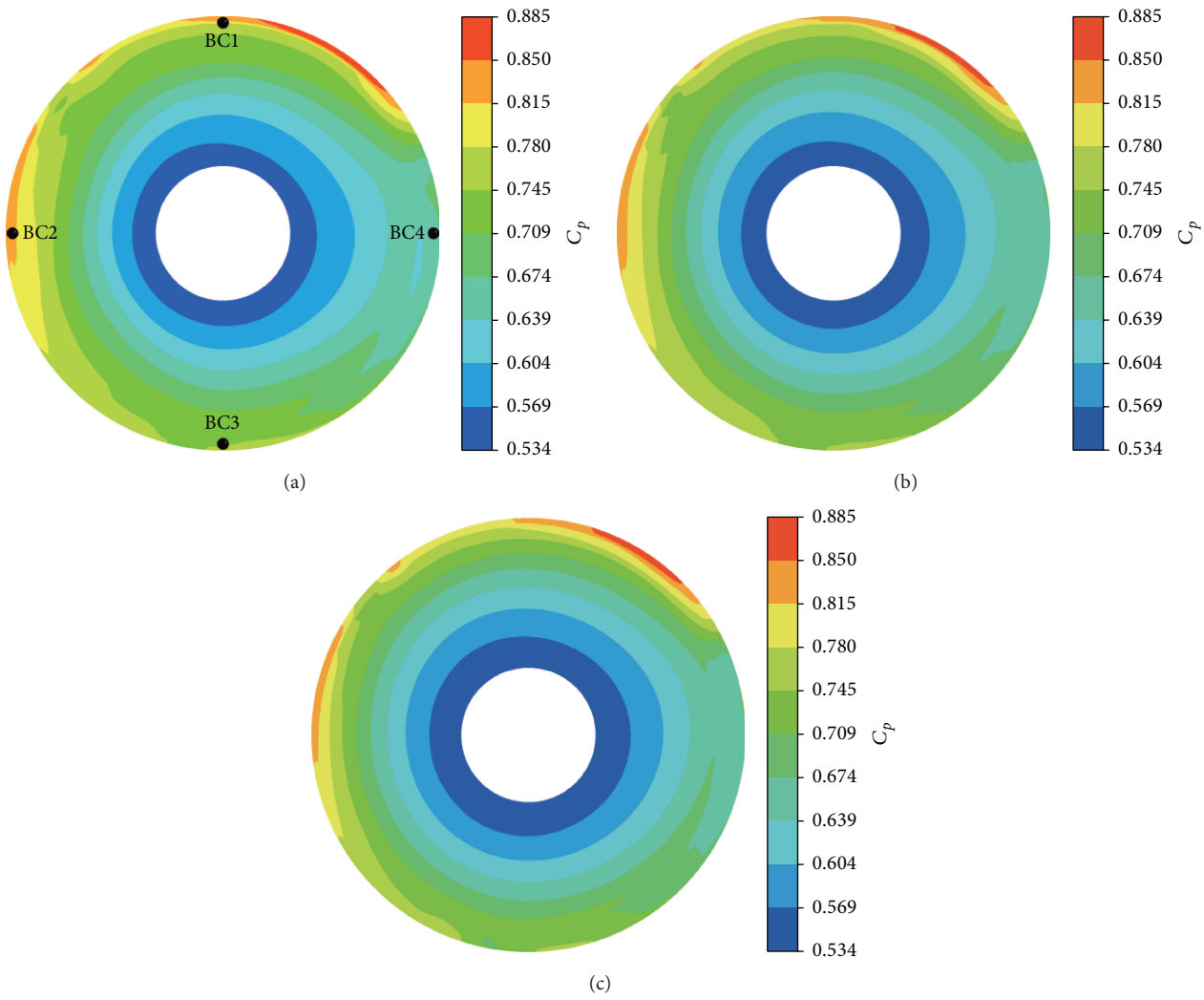

Figure 14: Pressure coefficient distribution on one section of the back sidewall gap at the last timestep: (a) M1, (b) M2, and (c) M3.

back shroud. Overall, clearance flows cannot be ignored and the axial clearance size has a certain influence on the pressure fluctuation characteristics in main flow domains as well as in sidewall gaps. The influence of the axial clearance on both pump performance and unsteady flow characteristics should be comprehensively considered in the hydraulic design of centrifugal pumps.

Competing Interests

The authors declared that there are no competing interests related to this paper.

Acknowledgments

The authors acknowledge the financial support given by the State Key Program of National Science of China (Grant no. 51439002), Special Funds for Marine Renewable Energy Projects (Grant no. GHME2012GC02), and State Key Laboratory of Hydroscience and Engineering (Grant no. 2014-KY-05).

References

[1] R. Dong, S. Chu, and J. Katz, "Effect of modification to tongue and impeller geometry on unsteady flow, pressure fluctuations, and noise in a centrifugal pump," *Journal of Turbomachinery*, vol. 119, no. 3, pp. 506–515, 1997.

[2] J. González, J. Fernández, E. Blanco, and C. Santolaria, "Numerical simulation of the dynamic effects due to impeller-volute interaction in a centrifugal pump," *Journal of Fluids Engineering*, vol. 124, no. 2, pp. 348–355, 2002.

[3] J. L. Parrondo-Gayo, J. González-Pérez, and J. Fernández-Francos, "The effect of the operating point on the pressure fluctuations at the blade passage frequency in the volute of a centrifugal pump," *Journal of Fluids Engineering*, vol. 124, no. 3, pp. 784–790, 2002.

[4] M. Kitano, "Numerical study of unsteady flow in a centrifugal pump," in *Proceedings of the ASME Turbo Expo 2004: Power for*

Land, Sea, and Air, vol. 5, pp. 805–814, Vienna, Austria, June 2004.

[5] J. González and C. Santolaria, "Unsteady flow structure and global variables in a centrifugal pump," *Journal of Fluids Engineering*, vol. 128, no. 5, pp. 937–946, 2006.

[6] J. González, J. Parrondo, C. Santolaria, and E. Blanco, "Steady and unsteady radial forces for a centrifugal pump with impeller to tongue gap variation," *Journal of Fluids Engineering*, vol. 128, no. 3, pp. 454–462, 2006.

[7] G. Pavesi, G. Cavazzini, and G. Ardizzon, "Time-frequency characterization of the unsteady phenomena in a centrifugal pump," *International Journal of Heat and Fluid Flow*, vol. 29, no. 5, pp. 1527–1540, 2008.

[8] R. Barrio, E. Blanco, J. Parrondo, J. González, and J. Fernández, "The effect of impeller cutback on the fluid-dynamic pulsations and load at the blade-passing frequency in a centrifugal pump," *Journal of Fluids Engineering*, vol. 130, no. 11, pp. 1111021–11110211, 2008.

[9] J. González, J. Manuel Fernández Oro, K. M. Argüelles Díaz, and E. Blanco, "Unsteady flow patterns for a double suction centrifugal pump," *ASME Journal of Fluids Engineering*, vol. 131, no. 7, Article ID 071102, 9 pages, 2009.

[10] S. Yuan, Y. Ni, Z. Pan, and J. Yuan, "Unsteady turbulent simulation and pressure fluctuation analysis for centrifugal pumps," *Chinese Journal of Mechanical Engineering*, vol. 22, no. 1, pp. 64–69, 2009.

[11] Z. Yao, F. Wang, L. Qu, R. Xiao, C. He, and M. Wang, "Experimental investigation of time-frequency characteristics of pressure fluctuations in a double-suction centrifugal pump," *Journal of Fluids Engineering*, vol. 133, no. 10, Article ID 101303, 2011.

[12] W. Wang and Y. Wang, "Analysis of inner flow in low specific speed centrifugal pump based on LES," *Journal of Mechanical Science and Technology*, vol. 27, no. 6, pp. 1619–1626, 2013.

[13] R. V. Uy and C. E. Brennen, "Experimental measurements of rotordynamic forces caused by front shroud pump leakage," *Journal of Fluids Engineering*, vol. 121, no. 3, pp. 633–637, 1999.

[14] R. Spence and J. Amaral-Teixeira, "Investigation into pressure pulsations in a centrifugal pump using numerical methods supported by industrial tests," *Computers & Fluids*, vol. 37, no. 6, pp. 690–704, 2008.

[15] S. H. Park and G. L. Morrison, "Centrifugal pump pressure pulsation prediction accuracy dependence upon CFD models and boundary conditions," in *Proceedings of the ASME Fluids Engineering Division Summer Conference (FEDSM '09)*, pp. 207–220, Vail, Colo, USA, August 2009.

[16] J. Pei, S. Yuan, F.-K. Benra, and H. J. Dohmen, "Numerical prediction of unsteady pressure field within the whole flow passage of a radial single-blade pump," *Journal of Fluids Engineering*, vol. 134, no. 10, Article ID 101103, 2012.

[17] J. Pei, S. Yuan, and J. Yuan, "Numerical analysis of periodic flow unsteadiness in a single-blade centrifugal pump," *Science China Technological Sciences*, vol. 56, no. 1, pp. 212–221, 2013.

[18] J. Pei, S.-Q. Yuan, J.-P. Yuan, and W.-J. Wang, "The influence of the flow rate on periodic flow unsteadiness behaviors in a sewage centrifugal pump," *Journal of Hydrodynamics*, vol. 25, no. 5, pp. 702–709, 2013.

[19] J. Pei, S. Yuan, X. Li, and J. Yuan, "Numerical prediction of 3-D periodic flow unsteadiness in a centrifugal pump," *Journal of Hydrodynamics*, vol. 26, no. 2, pp. 257–263, 2014.

[20] H. Liu, J. Ding, H. Dai, and M. Tan, "Investigation into transient flow in a centrifugal pump with wear ring clearance variation," *Advances in Mechanical Engineering*, vol. 6, Article ID 693097, 2014.

[21] J. W. Daily and R. E. Nece, "Chamber dimension effects on induced flow and frictional resistance of enclosed rotating disks," *Journal of Basic Engineering*, vol. 82, no. 1, pp. 217–230, 1960.

[22] B. Launder, S. Poncet, and E. Serre, "Laminar, transitional, and turbulent flows in rotor-stator cavities," *Annual Review of Fluid Mechanics*, vol. 42, no. 1, pp. 229–248, 2010.

[23] M. Piesche, "Investigation of the flow in the impeller-side space of rotary pumps with superimposed throughflow for the determination of axial force and frictional torque," *Acta Mechanica*, vol. 78, no. 3-4, pp. 175–189, 1989.

[24] B.-C. Will, F.-K. Benra, and H.-J. Dohmen, "Investigation of the flow in the impeller side clearances of a centrifugal pump with volute casing," *Journal of Thermal Science*, vol. 21, no. 3, pp. 197–208, 2012.

[25] ANSYS, *ANSYS CFX Modeling Guide*, ANSYS, 2015.

[26] Y. Zhang, *Research on centrifugal pump's working performance influenced by the gap variation between impeller and cover [M.S. thesis]*, Tsinghua University, Beijing, China, 2013.

[27] L. Cao, Y. Zhang, Z. Wang, Y. Xiao, and R. Liu, "Effect of axial clearance on the efficiency of a shrouded centrifugal pump," *Journal of Fluids Engineering*, vol. 137, no. 7, Article ID 071101, 2015.